Well-seismic bandwidth and time-lapse seismic characterization: physical considerations

Yinbin Liu, Don C. Lawton, and Gary F. Margrave

ABSTRACT

We discuss the physical aspects on well log integration with seismic and time-lapse seismic characterization for CO_2 injection based on a 1D thinly layered model. The results show that discrete layering and interval multiple reflections within sedimentary sequences have a significant influence on synthetic seismograms. The changes in reservoir velocity and density caused by CO_2 injection will mainly result in waveform distortions from the top of the reservoir to the base reflection near the reservoir. Large reservoir velocity changes may cause a time lag for the base reflection as well as deeper events. Those results have important implications for time-lapse seismic monitoring.

INTRODUCTION

Sonic logs and seismic surveys measure the acoustic responses of the earth with different resolutions. Sonic logs measure the interval transit time (reciprocal interval velocity) or waveform along a borehole section to identify lithology and pore fluids near the borehole with high resolution (tens of centimeters). A seismic survey measures the reflection traveling time (velocity) or waveform from subsurface to map structure, lithology, and pore fluids with low resolution (tens of meters). Physically speaking, seismic and sonic logs should be well integrated because they use same the physical method and measure “same thing”. For example, we may use the interval velocity and the density from logs to produce synthetic seismograms and then tie the seismic reflections at a well position. However, well-log-based synthetic seismograms usually do not agree well with observed seismic data, and stretching (occasionally squeezing) is required to get a good tie (e.g., White and Hu, 1998; Poggiagliomi and Allerd, 1996). There is a need to develop the physics to fill the gap between sonic bandwidth and seismic bandwidth so as to integrate well log and seismic data more thoroughly.

Time-lapse seismic data for geological storage of CO_2 and $CO_2-\mathrm{EOR}$ (enhanced oil recovery) operations show that there is a large “pushdown” effect or time sag caused by the CO_2 present above the reflectors (e.g. Jenkins, Waite, and Bee, 1997; Arts et al., 2004). There are complex chemical and physical interactions during CO_2 injection under reservoir condition that may cause a strong depth-dependent reservoir seismic heterogeneity. In order to simulate the heterogeneity produced by CO_2 injection, this work blocks the reservoir into many thin layers with depth-dependent impedance changes and then studies time-lapse seismic characterization.

We first study scale-dependent seismic reflection for a blocked up-wedge model. Then the interval multiple scattering for finely blocked well log data is analyzed. Finally the influence of the injected CO_2 on reservoir sonic velocity, and the corresponding time-lapse seismic characterization are discussed.

BANDWIDTHS

Well and seismic bandwidths

Sonic logs use ultrasonic transducers to generate pulse signals propagated along the borehole wall, and measure the internal transit time along the borehole section. The bandwidth of ultrasonic transducers for sonic logs is about 5 kHz to 30 kHz, and the distance between receivers is about 0.6 m for a compensated sonic tool and about 0.15 m for a dipole shear sonic tool (DSI). The sonic wavelength for a 15 kHz dominant frequency and a 3000 m/s internal velocity is 0.2 m. Therefore, sonic logs can usually identify individual sedimentary layers. Seismic surveys use dynamite or Vibroseis sources to generate seismic waves, and the reflected seismic signals are received by geophones. The bandwidth of seismic surveys is about 10 Hz to 120 Hz, and the corresponding seismic wavelength is tens of meters. A seismic reflector in a seismic reflection section is usually the overall response of an unconformity and many individual layers above and below the unconformity. Understanding the scale-dependent velocity dispersion and amplitude attenuation of seismic waves (well-seismic bandwidth) within sedimentary sequences is a key issue for subtle reservoir characterizations.

Frequency-dependent seismic reflections

Figure 1 is an up-wedge model (Hilterman, 2001) with a velocity from 2.25 km/s to 4.5 km/s over a 200 m depth. The corresponding densities range from 2.393 g/cm^3 to 2.8716 g/cm^3. The model can be approximately blocked into 20 transitional layers, each 10 m thick (the velocity increases in a step size of 0.1125 km/s and the density increases in a step size of 0.02393 g/cm^3). A propagator matrix method can be employed to study the reflection characterization for a thinly layered system. Figure 2 shows the calculated normal seismic reflection for a zero-phase Ricker wavelet source with different dominant frequencies (from 20 Hz to 400 Hz). The reflection waveforms in Figure 2 are polarity reversals because the reflections are from high to low impedance layers. It can be seen that seismic reflections are the accumulated effects of the transitional layers, and main waveform distortions are from a strong and abrupt contrast of acoustic impedance which is on the top boundary. It is difficult to identify the influence for the individual transitional layers for low frequency incident waves ($\lambda/d >$ about 2). However, the coda waves produced by reflection or scattering for high frequency incident waves ($\text{about } 2 > \lambda/d > \text{about } 0.8$) can be clearly seen. As λ/d decreases further ($\lambda/d <$ about 0.8), the later arriving reflections can be identified. Figure 3 shows the spectra of seismic reflections. Thin blue lines stand for the spectrum of the incident Ricker wavelet, and thick red lines stand for the spectra of reflection signals. It can be seen that spectral changes are small for low frequencies. However, there are very large spectrum changes for high frequency wavelets because of multiple scattering of waves.

Blocking

Most stratigraphy can be acoustically described by abrupt velocity (or lithology) changes between discrete strata. Figure 4 shows sonic and density logs from central

Alberta. The continuous log curves are the responses to geological character and should be blocked into discrete beds with constant velocity and density. The geological boundaries can be blocked by the positions of half-amplitude values in the log curve, and the measured maximum or minimum value within a blocked bed is taken as the corresponding velocity and density. The above processing is also physically reasonable because a seismic reflection is very sensitive to abrupt impedance changes. In this study we block the logs from 308 m to 2221 m into about 1350 layers. Figures 5 and 6 are the blocked density and velocity sections in the overburden and in the reservoir intervals respectively. It can be seen that the changes of density and velocity in the overburden are large. The large impedance contrasts may result in strong multiple scattering.

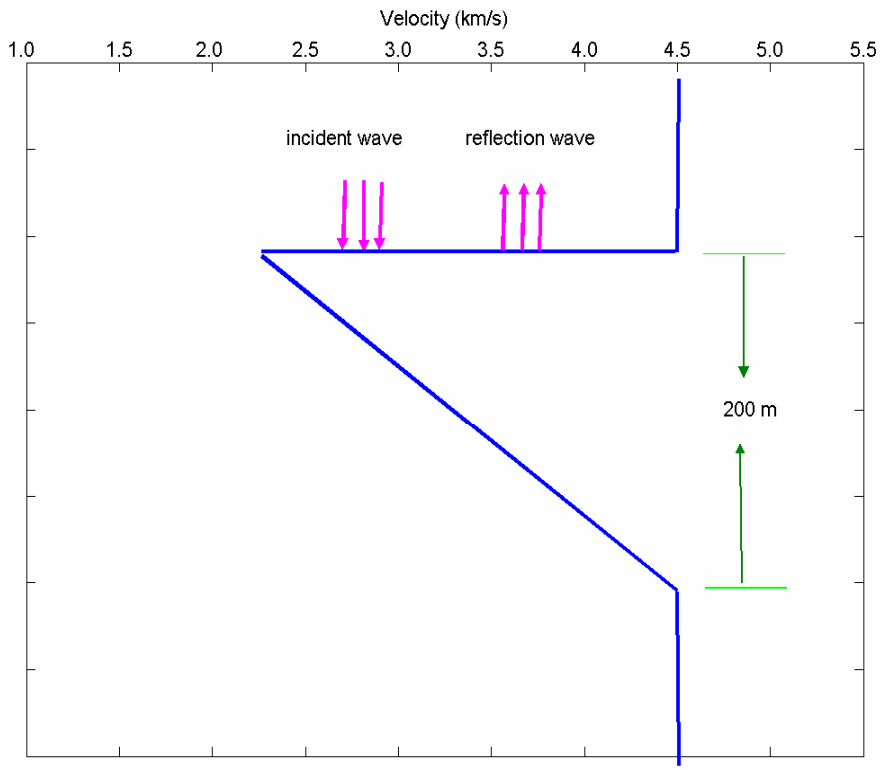

FIG. 1. An up-wedge model. The model is blocked into 20 transitional velocity layers, each 10 m thick (the velocity increases in steps of 0.1125 km/s).

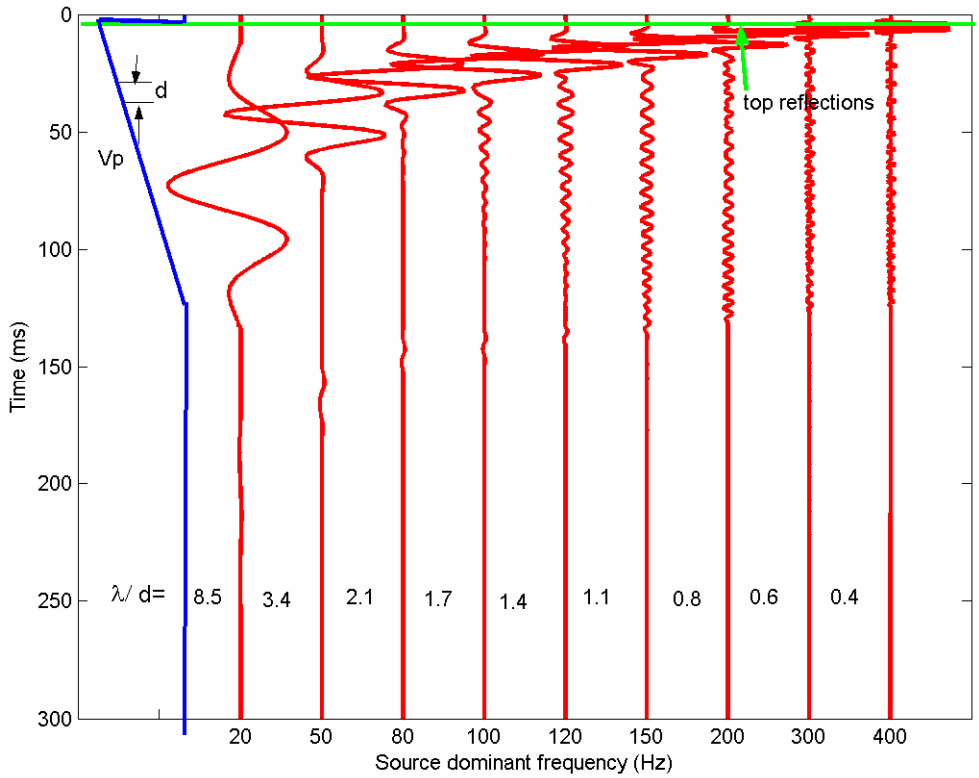

FIG. 2. Seismic reflections for the model in Figure 1.

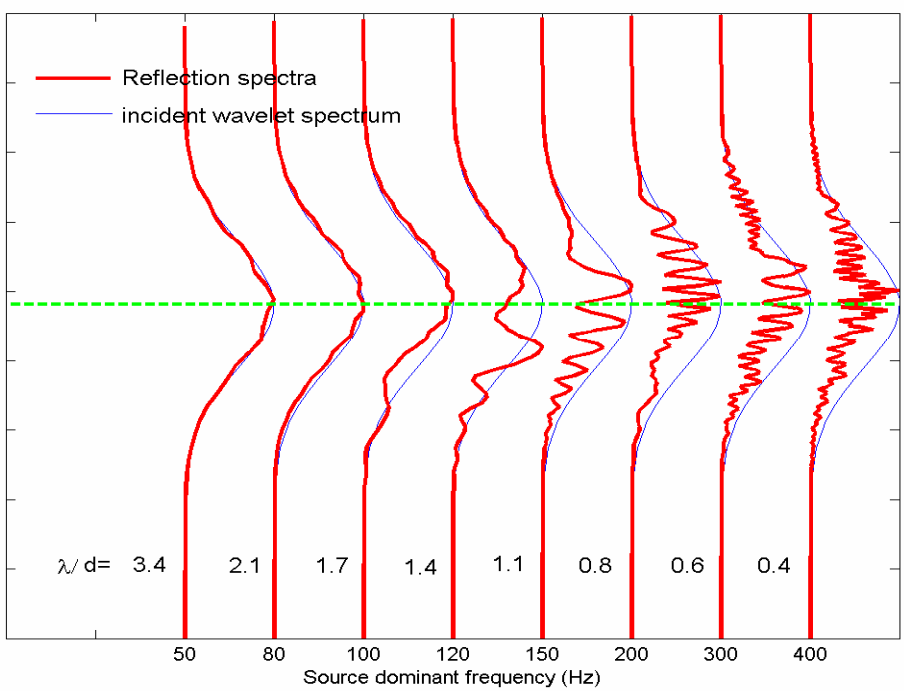

FIG. 3. Seismic reflection spectra of the traces in Figure 2.

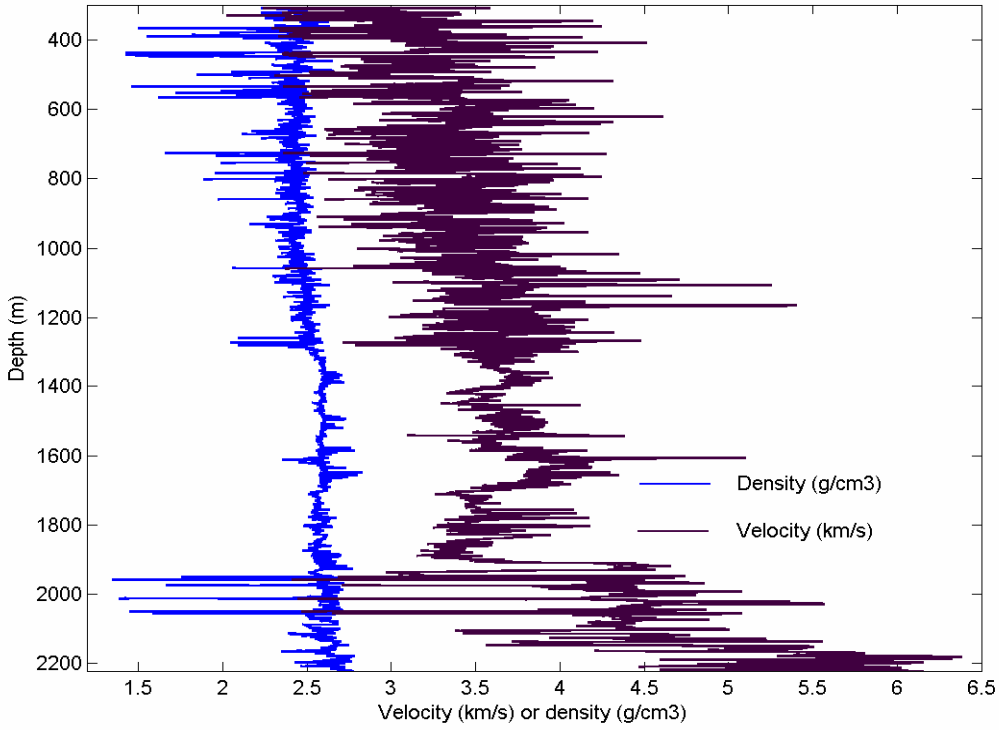

FIG. 4. Sonic and density logs from central Alberta.

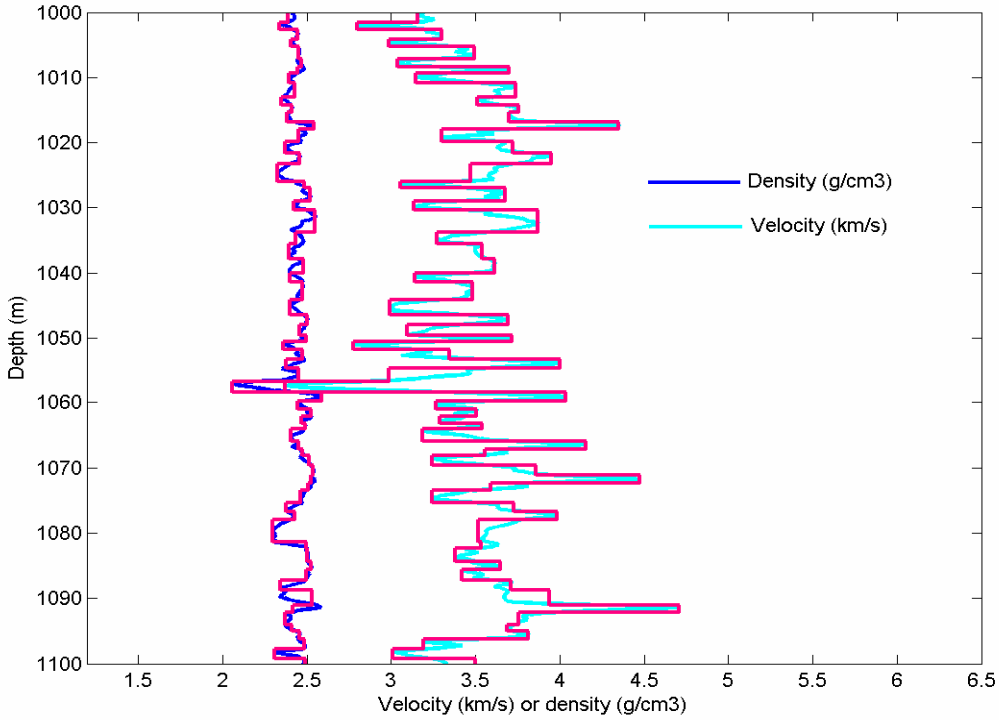

FIG. 5. Blocked density and sonic logs in the overburden section.

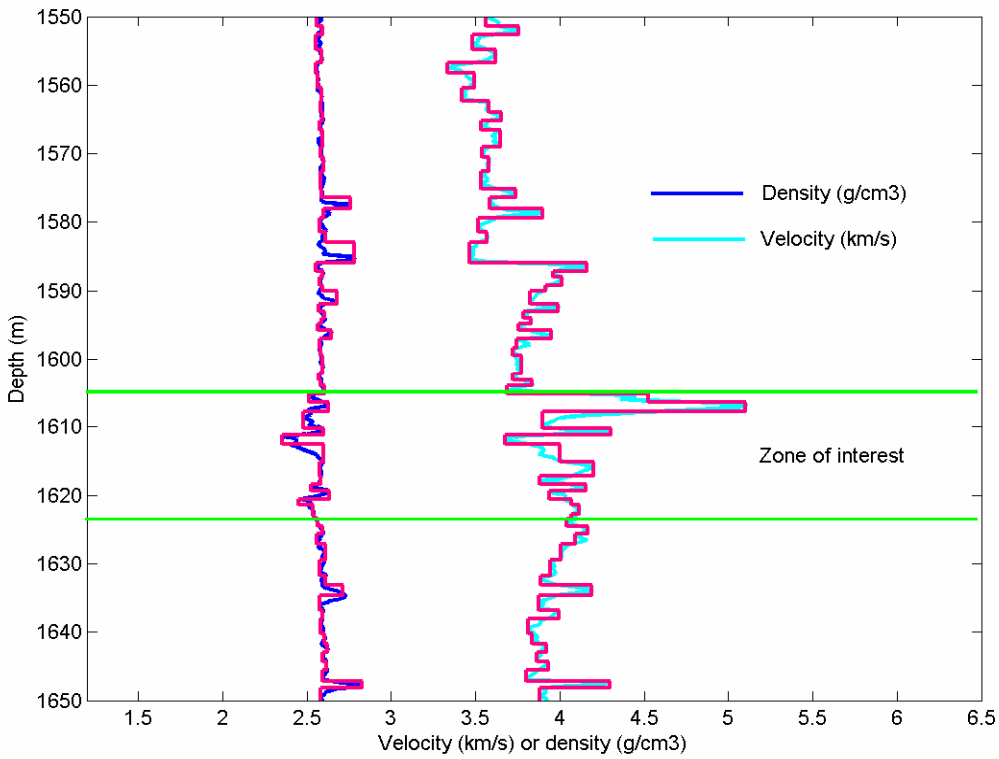

FIG. 6. Blocked density and sonic logs in the reservoir section.

Primary and multiples

The thickness of each blocked layer is usually much less than the seismic wavelength. The conventional convolution model based on the reflection coefficient of a single interface ($R = (\rho_2 v_2 - \rho_1 v_1)/(\rho_1 v_1 + \rho_2 v_2)$) will not completely describe the seismic reflection characterization for thinly layered sequences. The seismic multiple reflections (frequency-dependent reflection) may have a significant influence on the seismic signal. Figure 7 is the normal reflection synthetic seismogram calculated from the log data (about 1350 layers) in Figure 4. The blue and red lines stand for the results from primary reflections (conventional convolution model) and multiple reflections (propagator matrix, which includes both primary and multiples), respectively. It can be seen that there is a large difference between the primary and multiple synthetic seismograms. The larger the propagation time or distance, the larger is the waveform difference. Figure 8 reproduces the seismic reflections in Figure 7 for the arrival times from 1100 ms to 1400 ms. The amplitude difference at about 1300 ms between the primary and multiple synthetic seismograms is up to about 500%. This is because a long propagation time or traveling distance will include more multiple waves. The interference of multiple waves may result in large changes in amplitude, frequency, and phase or time. Therefore, the multiple reflections must be included in the generation of synthetic seismograms.

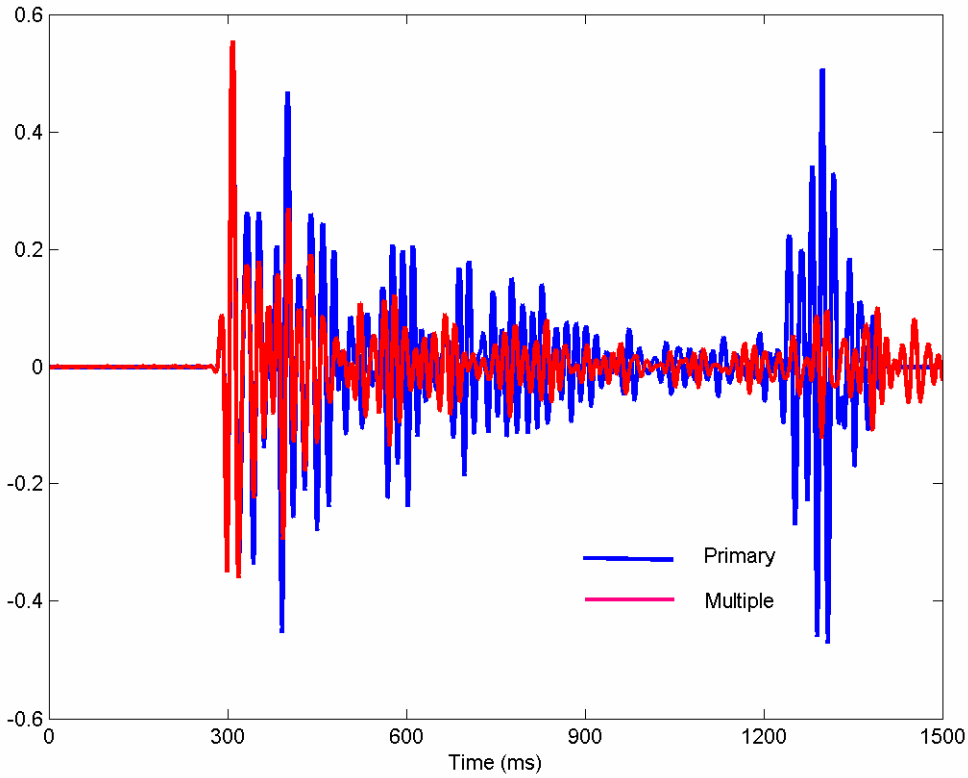

FIG. 7. Primary (blue) and multiple (red) synthetic seismograms.

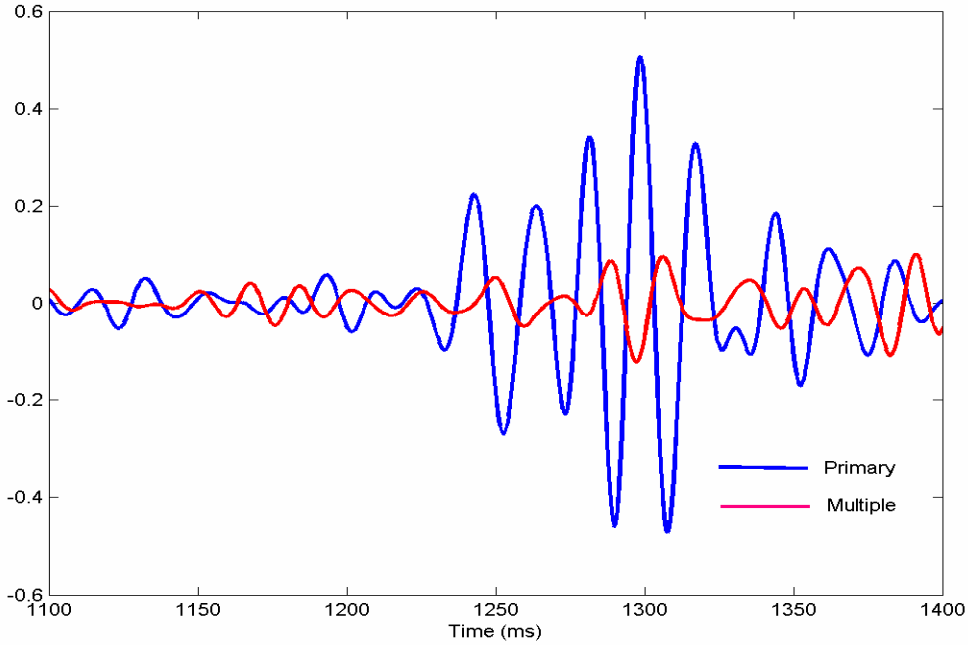

FIG. 8. There is a large difference between the primary (blue) and multiple (red) synthetic seismograms.

SEISMIC VELOCITY IN POROUS MEDIA

Acoustic property of CO_2

Subsurface storage of CO_2 is seen as a key mechanism for reducing the emission of greenhouse gases into the atmosphere. As gaseous CO_2 is injected into the subsurface it undergoes increases in both sonic velocity and density associated with a phase change from gas to liquid or supercritical fluid because of the changes of temperature and pressure (Figure 9). The acoustic property of a mixture of gaseous CO_2 and fluid is much different from either the fluid or gaseous CO_2 (Kieffer,1977). Figure 10 shows the sound velocity of a water and gaseous CO_2 mixture at standard condition (immiscible, 25^0 degree and 0.1 Mpa). It can be seen that very small concentrations of gaseous CO_2 may dramatically reduce the sound velocity. The velocity of a water and gaseous CO_2 mixture is only about 24 m/s for gaseous CO_2 for concentrations from 10% to 90%. This is because the two-phase system has the compressibility of a gas but a density defined by the fraction of liquid.

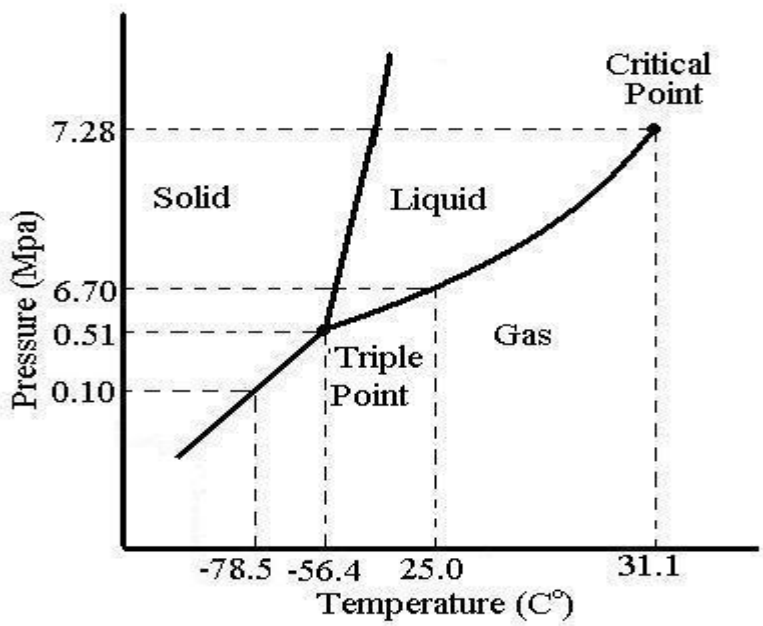

FIG. 9. Phase diagram for CO_2 (not to scale).

Ideal conditions for subsurface storage of CO_2 are usually at depths of about 1000 m or deeper, where CO_2 is in the supercritical state (Figure 9). At the study site for CO_2 injection (Penn West site), the pressure is about 19 MPa and the temperature is 50^0 C for CO_2 injection into the formation. At these pressure and temperature conditions,

supercritical CO_2 behaves still like a gas by filling all the available volume, but has a "liquid" density that increases, depending on pressure, temperature and water salinity. The injected CO_2 will mix with the water, oil, and brine under reservoir condition. The theoretical and experimental results show that the supercritical CO_2 has little influence on the fluid acoustic properties because the injected CO_2 is dissolved in the fluids under this condition (Kieffer, 1977).

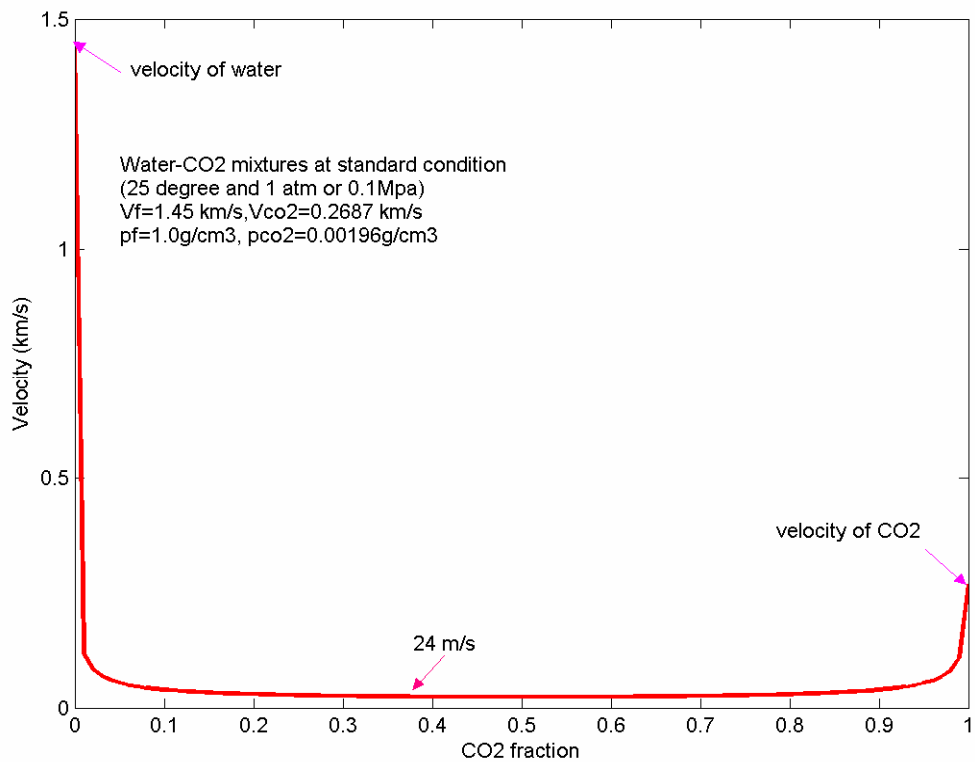

FIG. 10. Sonic velocity of a mixture of water and CO_2 under standard condition.

Gassmann's fluid substitution

Gassmann's fluid substitution equation is usually employed to study the influence of water saturation on reservoir acoustic velocity (e.g., Mavko et al., 1998; Han and Batzle, 2002; Calvert, 2005). Figure 11 shows the calculated Gassmann's fluid substitution velocities for a 15% porosity sand for different CO_2 saturations. The coloured lines stand for four acoustic velocities and densities of CO_2, which simulates different reservoir pressures and temperatures. It can be seen that the seismic velocity is nearly independent of the CO_2 saturation when the CO_2 saturation is higher than about 20%, and the velocity change is still not large for most low CO_2 saturations (< 20%). The velocity only reduces to about 80% the original velocity even if the injected CO_2 is in gaseous state (for example, V_{co2} = 0.5 km/s and ρ_{co2} = 0.1 g/cm^3). The above properties given by Gassmann's equation suggest that seismic techniques can not be used to identify CO_2

saturation and distribution, and the difference for time-lapse seismic data should be small (small velocity change from Gassmann's equation). However, real data show that the "pushdown" effect or time sag will increase with the amount of injected CO_2, and there are large amplitude anomalies for time-lapse seismic surveys. This means that further work is needed for saturation models (e.g., Jenkins et al., 1997; Arts et al., 2004).

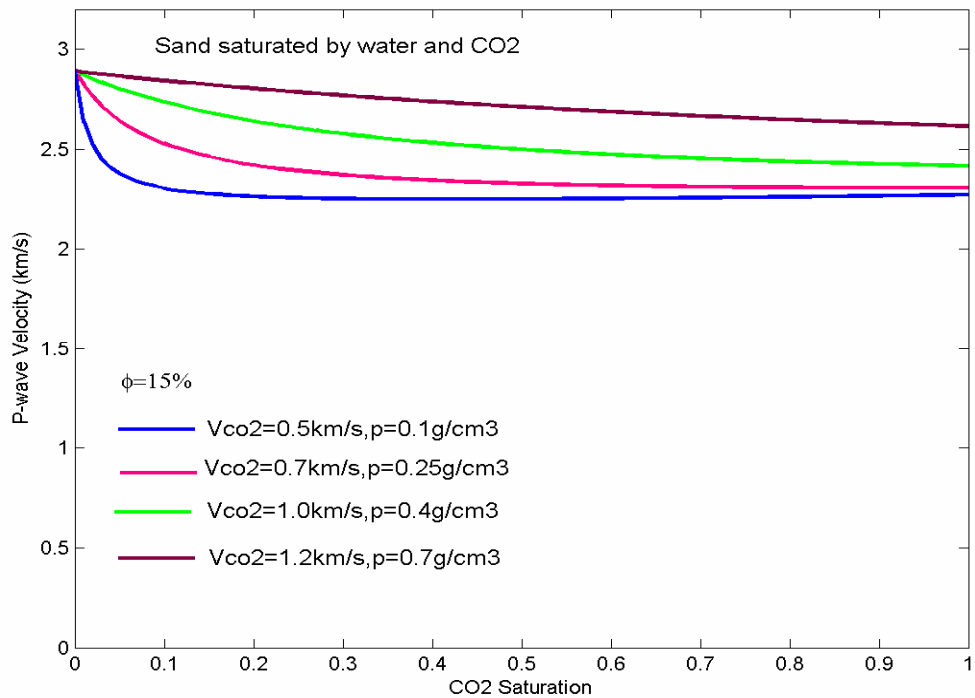

FIG. 11. Gassmann's fluid substitution for four kinds of CO_2 velocities and densities.

CO_2 injection model

The thickness of the reservoir sand in the studied area is about 18.5 m (depth from about 1605 m to 1623.5 m), which is blocked into 14 thin layers in Figure 6 (the thickness of each blocked layer is much less than the seismic wavelength). CO_2 injection will cause complex physical and chemical reactions which are still research projects. Small concentrations of gas or vapor bubbles produced by $CO_2 - \mathrm{EOR}$ operations might have a very important influence on fluid acoustic properties as discussed in Figure10. The injected CO_2 tends to move up and first substitutes (or dissolves with) the original pore fluids at the top of the reservoir. Thus the changes of velocity and density produced by CO_2 injection are strongly non-uniform and tend to decrease with depth as shown in the up-wedge model (Figure 1). This kind of depth-dependent heterogeneity can be incorporated into a 1D layered model by blocking the reservoir into many thin layers. The strong heterogeneity at the top of the reservoir produced by CO_2 injection is simulated by thin layers with large impedance contrasts (for example, 50% velocity

changes). In the following we numerically study the influence of the changes of the reservoir velocity and density on the time-lapse seismic reflections.

TIME-LAPSE SYNTHETIC SEISMIC RESPONSES

Figure 12 models the influence of reservoir velocity changes on seismic reflections (the influence of the injected CO_2 on density is first ignored in Figure 12). The reservoir velocity changes to 70% of the original reservoir velocity. The red lines stand for a seismic reflection based on the original reservoir velocity, and the blue, green, and black lines stand for seismic reflections at five reduced reservoir velocities, respectively. It can be seen that the reservoir velocity changes will result in changes of seismic reflections both from and below the reservoir. This is because the seismic reflections from below the reservoir section are also affected by the reservoir. The waveform distortions in amplitude, frequency, and phase both from and below the reservoir sections carry the information on CO_2 saturation and distribution. This suggests that the injected CO_2 distribution can be detected from not only the reservoir section but also below the reservoir section.

Figure 13 reproduces the seismic reflection in Figure 12 at the arrival times from 1000 ms to 1400 ms. The top reservoir reflection is at about 1060 ms and the base reflection near the reservoir (BNR) is at about 1280 ms. It can be seen that both the overall differences of seismic reflections and the amplitudes of the top reservoir reflection increase with the reservoir velocity changes because of increased impedance contrasts. The time sags or “pushdown” effect from the base reflections for large reservoir velocity changes (>80%) can be clearly seen because of the low propagation velocity in the reservoir section. The waveform distortions mainly take place in the section from the top reservoir to the base reflection near the reservoir. Figure 14 shows a cartoon to explain the multiple scattering from the reservoir. The multiple reflection and scattering waves both from the top and bottom of the reservoir and within the reservoir will mainly accumulate in the section from the top reservoir to the BNR and form coda waves, which are related to the level and distribution of CO_2. The influence of the reservoir on the base reflection will mainly occur as time sags (passing the reservoir twice) as observed by many case studies (e.g., Jenkins, Waite, and Bee, 1997, Calvert, 2005). This suggests that the seismic reflections (or coda waves) from the top of the reservoir to the base near the reservoir (BNR) and the time sag from the base reflection as well as deeper events may be used for time-lapse seismic monitoring.

Figures 15 shows the influence of gradually changed reservoir velocity and density (both velocity and density changes are similar to Figure 1) on seismic reflections for 5 different reservoir thicknesses. From the top to the bottom of the reservoir the velocity changes from 80% to 100% of the original reservoir velocity, and the density changes from 90% to 100% of the original reservoir density. The red lines stand for a seismic reflection from the original reservoir velocity and density. The blue lines stand for seismic reflections from the five altered reservoirs. It can be seen that the differences of seismic reflections increases with the injected reservoir thickness (or amount of CO_2 injection). A thin CO_2 injected layer will mainly change the amplitude of a seismic

reflection while a thick CO_2 injected layer will change the waveform of a seismic reflection (amplitude, frequency, and phase).

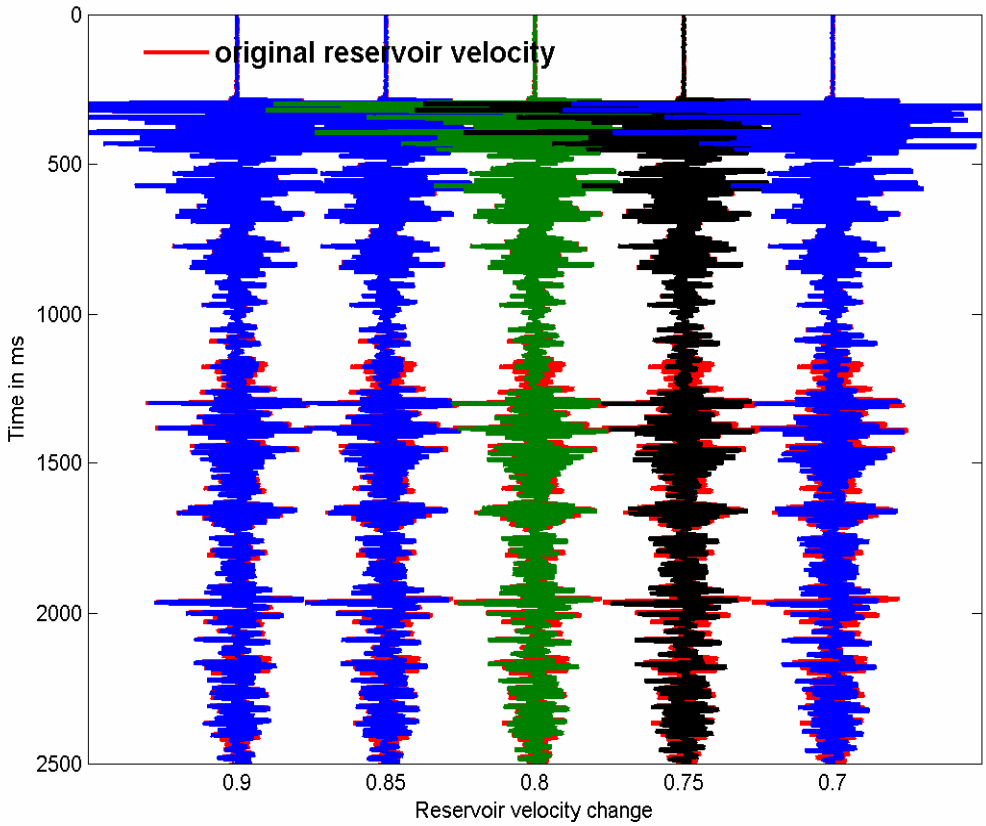

FIG. 12. The influence of reservoir velocity on seismic reflections. The red lines stand for a seismic reflection from the original reservoir velocity and the blue, green, and black lines stand for seismic reflections from five reduced reservoir velocities, respectively.

In order to study the influence of a strong reservoir heterogeneity produced by CO_2 injection on time-lapse seismic, Figure 16 shows the influence of the large gradually changed reservoir velocity and density on seismic reflection for 5 different reservoir thicknesses (or amount of CO_2 injection). The velocity changes from the top to the bottom of the reservoir range from 50% to 100% of the original reservoir velocity, and the density changes range from 80% to 100% of the original reservoir density. It can be seen that both, the waveform distortion from the top reservoir to the BNR, and the time sag from the BNR, are much larger than those of Figure 15.

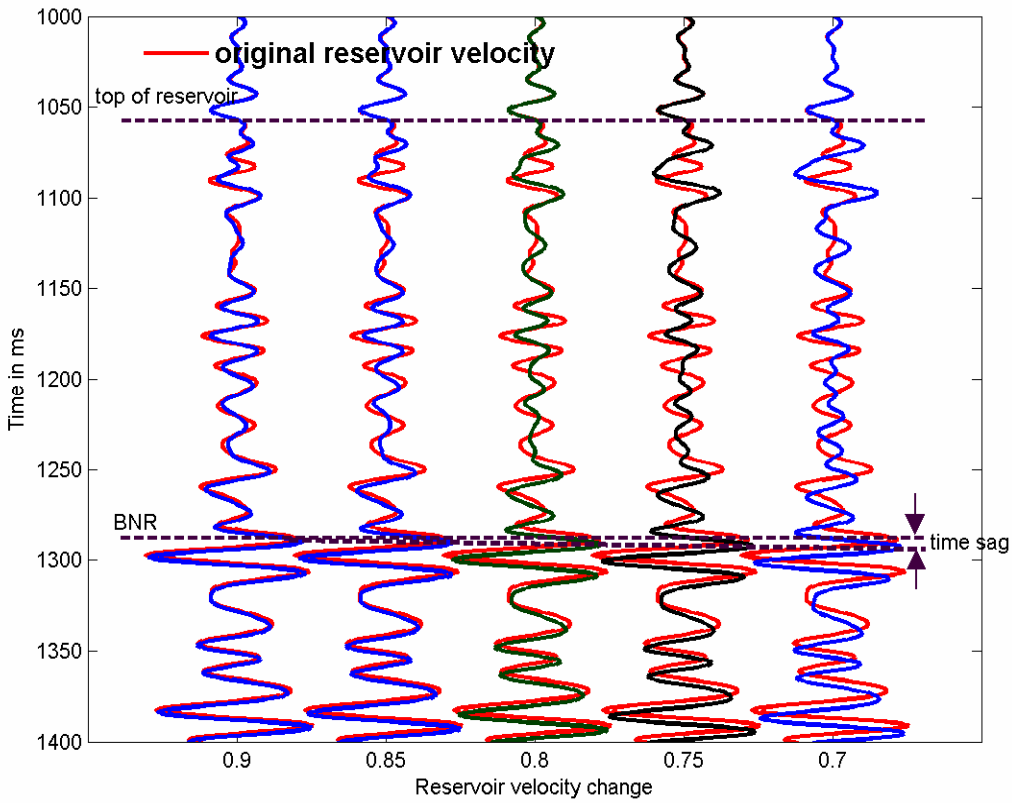

FIG. 13. The difference between seismic reflections increases with reservoir velocity changes.

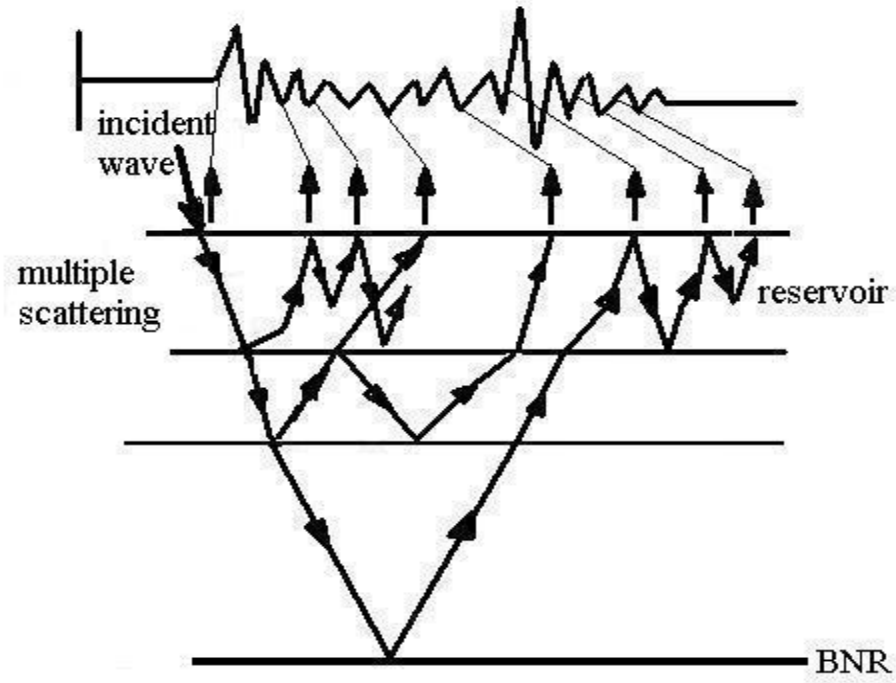

FIG. 14. Multiple scattering from the reservoir and the base near the reservoir.

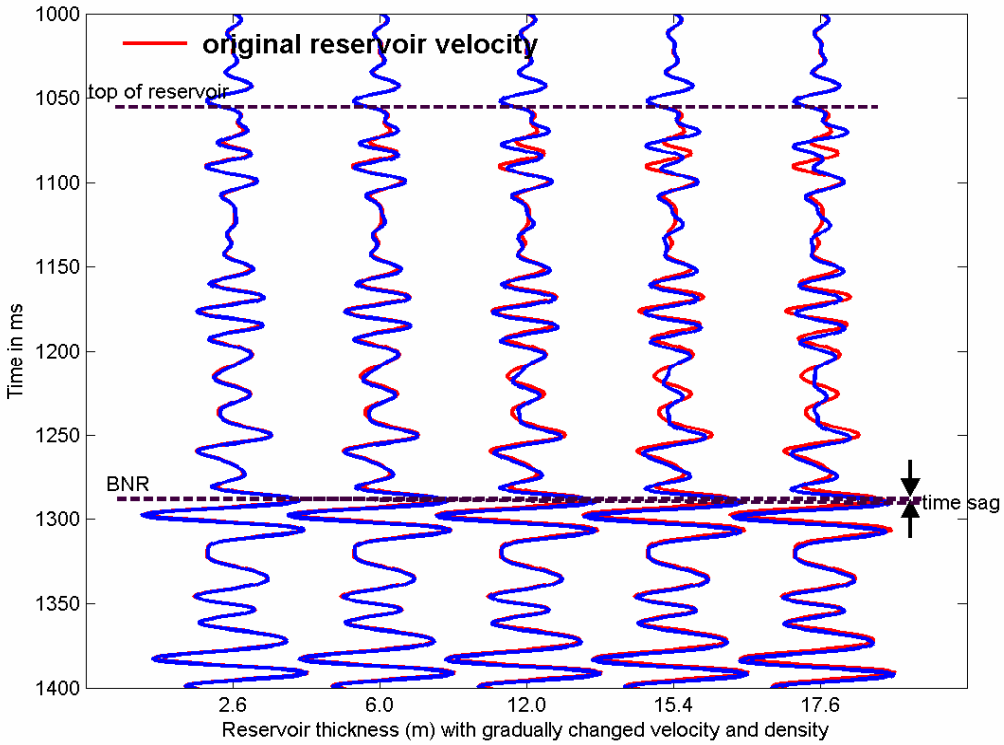

FIG. 15. The difference between seismic reflections increases with reservoir thickness.

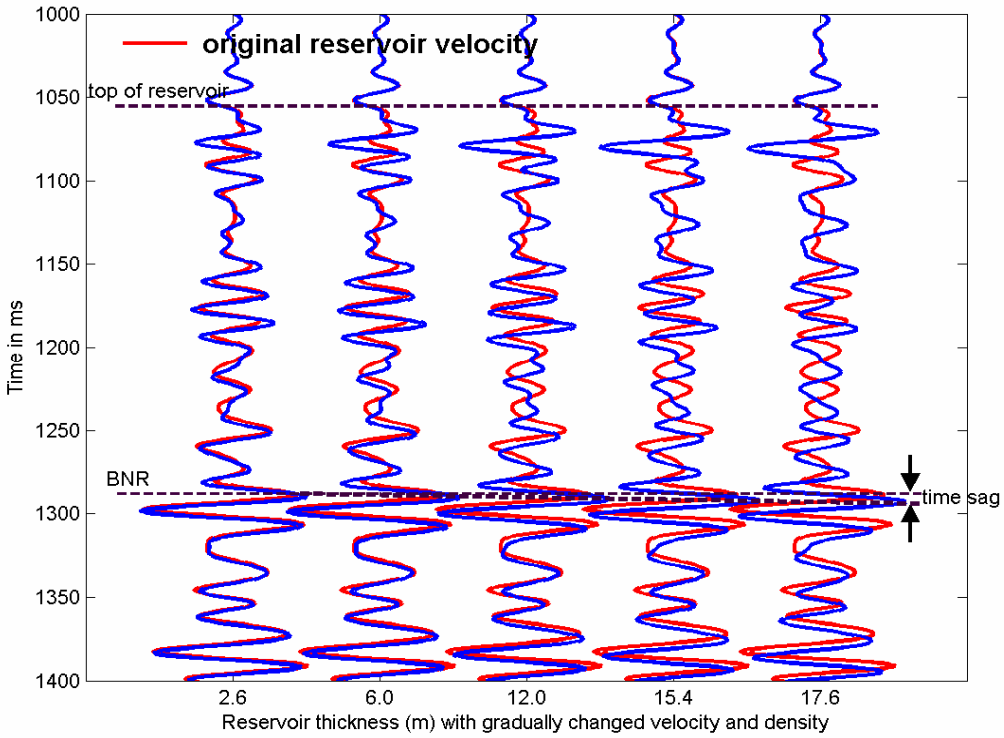

FIG. 16. Same as Figure 15, except with larger reservoir impedance changes.

DISCUSSION AND CONCLUSIONS

The time-lapse seismic reflection characterization of CO_2 injection is studied based on a 1D thinly layered model. The injected CO_2 causes changes of seismic reflections both from and below the reservoir. The waveform distortions and coda waves produced by interval multiple scattering will mainly take place in the section from the top reservoir to the base reflection near the reservoir, which is related to the saturation and distribution of the injected CO_2. Time-lapse seismic anomalies cannot be explained completely by Gassmann's fluid substitution, and further work on saturation models is needed. Seismic AVO analysis of the reflections from the top of the reservoir to the BNR (both scale-dependent and angle-dependent seismic multiple scattering for a thinly layered system) may possibly provide useful clues for the determination of distributions and levels of CO_2.

ACKNOWLEDGEMENTS

The authors thank for the support of the CREWES project in the Department of Geology and Geophysics, University of Calgary, and from NSERC.

REFERENCES

Arts, R., O. Eiken, O., Chadwick, A., Zweigel, P., Van Der Meer, B., and Kirby, G., 2004, Seismic monitoring at the Sleipner underground CO_2 storage site (North sea): Geological Storage of Carbon Dioxide, Eds: S. J. Baines and R. H. Worden, 181-191, Geological Society.

Calvert, R., 2005, Insights and Methods for 4D Reservoir Monitoring and Characterization: 2005 SEG/EAGE Distinguished Instructor Short Course.

Han, De-Hua, Batzle, M., 2002, Fizz water and low gas-saturated reservoirs, The Leading Edge, **21**, 395-398.

Hilterman, F. J., 2001, Seismic Amplitude Interpretation: 2001 SEG/EAGE Distinguished Instructor Short Course.

Jenkins, S. D., M. W. Waite, and M. F. Bee, 1997, Time-lapse monitoring of the Duri steamflood: A pilot and case study: The Leading Edge, **16**, 1267-1273.

Kieffer S. W., 1977, Sound speed in liquid-gas mixtures: water-air and water-steam: Journal of Geophysical Research, **82**, 2895-2904.

Mavko, G., Mukerji, T., and J. Dvorkin, 1998, The rock physics handbook: Cambridge University Press.

Poggiagliolmi, E. and R. D. Allerd, 1996, Detailed reservoir definition by integration of well and 3-D seismic data using space adaptive wavelet processing: Seismic Source Signature Estimation and Measurement, Eds: O. M. Osman and E. A. Robinson, 571-576, SEG.

White, R. E. and T. Hu, 1998, How accurate can a well tie be: The Leading Edge, **17**, 1065-1071.